

## Quantification of Dendritic Cells entering the Lymph Nodes in Mice using $^{19}\text{F}$ MRI

Conrad Steven Martin<sup>1</sup>, Min-Chi Ku<sup>1</sup>, Stefano Lepore<sup>1</sup>, Helmar Waiczies<sup>1,2</sup>, Andreas Pohlmann<sup>1</sup>, Jan Hentschel<sup>1</sup>, Matthias Dieringer<sup>1,2</sup>, Thoralf Niendorf<sup>1,2</sup>, and Sonia Waiczies<sup>1,3</sup>

<sup>1</sup>Berlin Ultrahigh Field Facility (B.U.F.F.), Max Delbrück Center for Molecular Medicine, Berlin-Buch, Berlin, Germany, <sup>2</sup>MRI TOOLS GmbH, Berlin, Germany, Berlin-Buch, Berlin, Germany, <sup>3</sup>Experimental and Clinical Research Center, Berlin, Germany, Berlin-Buch, Berlin, Germany

### Introduction:

Fluorine-19 ( $^{19}\text{F}$ ) can be used for the labeling and tracking of cells in living organisms using MRI. Perfluorocompounds (PFC) are very stable; however they are lipophilic and need to be emulsified to be taken up by phagocytes. Following labeling,  $^{19}\text{F}$ -labeled cells can be applied *in vivo* to follow their movement over a period of several days or even weeks. With the advent of high field MRI, and with the corresponding increase in signal sensitivity it is possible to track even small numbers of cells in very specific locations *in vivo* [1]. In this work the goal was to quantify numerically and temporally the movement of mouse dendritic cells (DCs) to the popliteal lymph nodes after intradermal injection. This is relevant to immunological research since it gives a longitudinal understanding of DC migration *in vivo*. DC migration has commonly been studied in cross-sectional studies. By studying the longitudinal behavior of DCs *in vivo*, as well as ways and means how this behavior could be manipulated, attempts are created to deliver effective human DCs vaccines in tumor and infectious disease.

### Method:

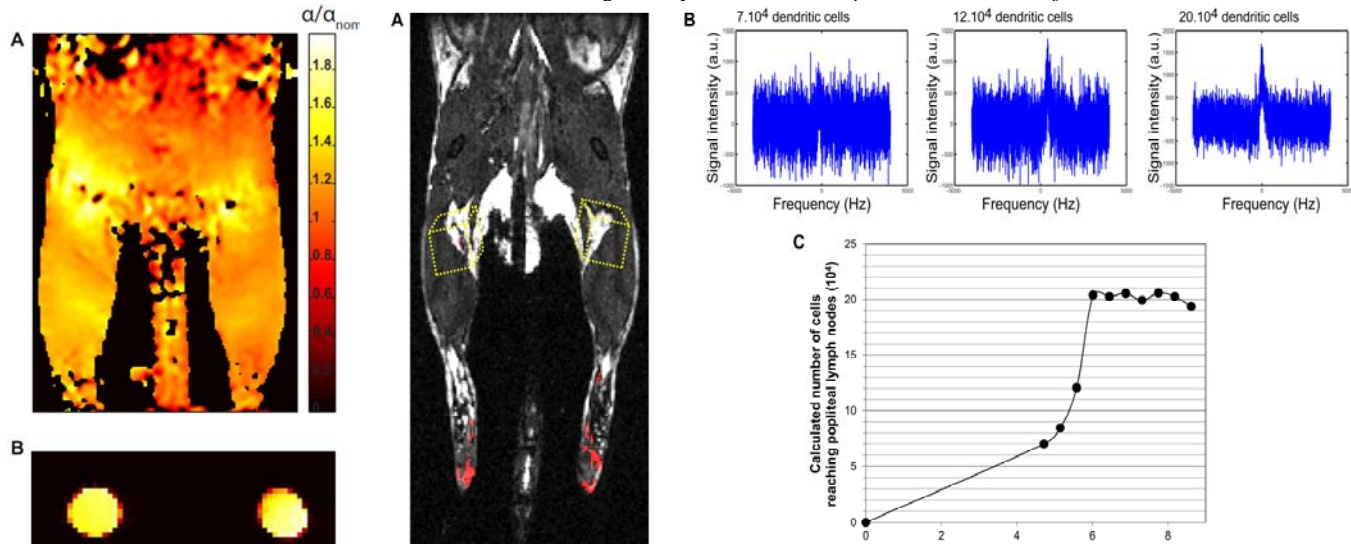
DCs were generated from bone marrows of C57BL/6 mice as previously described [2]. Nanoparticles containing Perfluoro-15-crown-5-ether (PFCE) were produced in a size range of 300-350 nm. These nanoparticles were applied to DC cultures on day 9 (10  $\mu\text{mols}$  of  $^{19}\text{F}$  per culture plate equivalent to approximately  $10^7$  cells), which resulted in a quantity on the order of 3 to 10 nmols of  $^{19}\text{F}$  per million cells. These cells were matured overnight using lipopolysaccharide and harvested on day 10 of the cell culture, then injected intradermally into the footpads of mice (5 to 10 million cells per footpad). The mice were subsequently scanned in a 9.4 Tesla small bore scanner (Bruker Biospin, Ettlingen, Germany) equipped with a 35 mm  $^{19}\text{F}/^1\text{H}$  RF coil. Phase cycled balanced steady state free precession (bSSFP, 1 average, TE=1.772 ms, TR=3.595 ms, scan time=1:02, 4 phase cycles) scans were performed to achieve high contrast images of the lower limb, importantly to distinguish the popliteal lymph nodes from the surrounding tissue. Point resolved  $^{19}\text{F}$  spectroscopy (PRESS, TE = 11.64 ms, TR = 1500 ms, voxel size (5x5x5) mm<sup>3</sup>, NEX= 512, scan time = 13:54min. Voxels were placed on the popliteal lymph nodes after voxel based  $B_0$  shimming was performed.  $^{19}\text{F}$  PRESS measurements were conducted between 3 and 8 hours after injection. For calibration of the *in vivo* scans  $^{19}\text{F}$  spectroscopy was conducted with a known number of cells from the cell culture in order to determine the exact concentration of fluorine in the cells. A plot is constructed of the numbers of cells in each  $^{19}\text{F}$  PRESS voxel scan vs. the amount of time after injection. To assure correct flip angles for  $^{19}\text{F}$  PRESS, normalized radio frequency transmission field ( $B_1^+$ ) maps were acquired using the double angle method ( $\alpha_1=45^\circ$ ,  $\alpha_2=90^\circ$ , slice thickness=7 mm, TE=2.8 ms, TR=7000 ms, scan time=7:30 min).

### Results:

Coronal and axial  $B_1^+$  maps show rather uniform  $^{19}\text{F}$  transmission field uniformity as demonstrated Figure 1A and 1B. Mean  $B_1^+$  deviation between left and right legs was  $1.5\pm 0.1$  and  $1.4\pm 0.1$  respectively (normalized values), which allows a comparison. An overlay of both  $^{19}\text{F}$  (red) and  $^1\text{H}$  (gray scale) bSSFP images indicates the spatial distribution of  $^{19}\text{F}$  labeled DC and the anatomy of the lower limb, respectively (Figure 2A). Typical spectral peaks of the  $^{19}\text{F}$  signal from PRESS voxel scans of lymph nodes are shown in Figure 2B. The threshold of detection in the PRESS voxel scans lies at approximately 10,000 cells (Figure 2B), depending on the unique concentration of PFCE taken up by the cells from that specific culture. Due to biological reasons, only a small percentage of the applied DCs actually reach the popliteal lymph nodes 5-6 hours after injection (standard deviation of 1.5 hours) as illustrated in Fig. 2C. The cell movement to the popliteal lymph node usually reaches a maximum at 250,000 cells (standard deviation of 150,000 cells) approximately 7-9 hours after injection. After this point the cell concentration in the lymph nodes decreases until after 72 hours no more  $^{19}\text{F}$  signal is detectable on the bSSFP scans. At this point the cells most likely have either moved beyond the popliteal lymph nodes to other lymph node stations, or the cell debris are metabolized via the reticuloendothelial system.

### Discussion and Conclusions:

Our results demonstrate that it is feasible to track and quantify the movement of  $^{19}\text{F}$ -labeled DCs *in vivo* in mice over a period of several hours and even days. Although the standard deviations of the number of cells observed and of the timeframe in which they were observed is quite large, their consistency is sufficient to make distinctive claims about the cellular movement of DCs *in vivo*. Given a sufficiently large sample size, experiments can be done using this procedure to test cell types with various genetic and biochemical modifications for their mobility and direction *in vivo*. This will be extremely useful in immunological studies involving the genetic and chemical modifications of human cells for the treatment of various tumor diseases such as Glioma, which cannot easily be reached by surgical or chemotherapeutic means. Although there is always a significant degree of variation in the biological functions of different animals *in vivo*, it is possible to improve the consistency of the cellular motion observation with more sensitive scanning equipment, and by gaining more precise and consistent control of culturing techniques, nanoparticle production techniques, and injection procedures. Such a reduction in procedural variables would benefit the accuracy to determine the effect of various cellular modifications on their resulting mobility and accumulation points inside of test subjects.



**Figures 1:**  $B_1^+$  Map. This  $B_1^+$  Map of the coronal (A) and axial (B) view of the mouse legs at the height of the popliteal lymph nodes shows that the  $B_1$  field generated by the  $^{19}\text{F}$  coil has only minor discrepancies in its intensity from left to right. This indicates that the data from both sides are comparable.

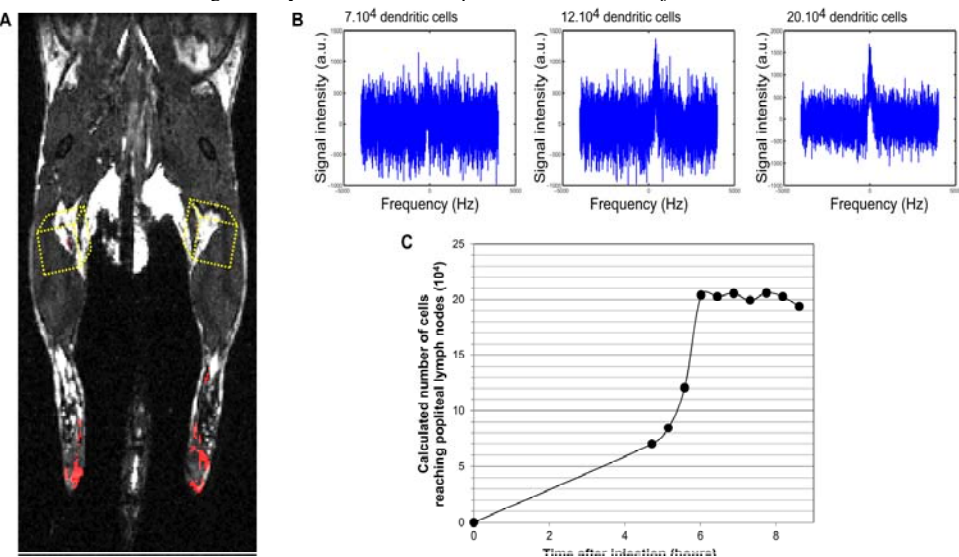


**Figure 2:** Localization and calculation of DC numbers in the draining lymph node. (A) Following injection of  $10^7$  dendritic cells in the foot pad, a visual overview of the cellular movement can be made. Shown is a composite image of the  $^1\text{H}$  balanced SSFP scan (gray) with the  $^{19}\text{F}$  bSSFP scan (red). PRESS voxels are placed around the lymph node (yellow dashed cube) to determine the  $^{19}\text{F}$  signal in these PRESS voxels. In this particular image, 26,600 cells can be seen at the lymph node, which is the approximate minimum number of detection in this setup. (B)  $^{19}\text{F}$  PRESS spectra representative of 70 (left), 120 (center) and 200 (right) thousand cells 4.7, 5.6 and 6 hours after injection, respectively, calculated by using the amount of  $^{19}\text{F}$  signal derived from our calibration curve (see Method). (C) A graph of the number of cells arriving at the lymph nodes over time, after injection into the footpads.

### References:

/1/ Waiczies H, et al. PLoS One. 2011. V6 (7):e21981  
 /2/ Waiczies H, et al. Journal of Visualized Experiments. 2013. DOI:10.3791/50251